1983ApJ...274..677P

THE ASTROPHYSICAL JOURNAL, 274:677–697, 1983 November 15
© 1983. The American Astronomical Society. All rights reserved. Printed in U.S.A.

CENTRIFUGALLY DRIVEN WINDS FROM CONTRACTING MOLECULAR DISKS

R. E. PUDRITZ
Institute of Astronomy, Cambridge; and Astronomy Department and Space Sciences Laboratory, Berkeley
AND
C. A. NORMAN
Institute of Astronomy, Cambridge; and Sterrewacht, Huygens Laboratory, Leiden
Received 1982 September 7; accepted 1983 April 21

ABSTRACT

We suggest that bipolar outflows in dense molecular clouds associated with young stellar objects are steady, centrifugally driven, hydromagnetic winds that arise from molecular disks (on scales $\leq 10^{16}$ cm) in which the infrared source(s) is embedded. A disk of mass $\sim 100\ M_\odot$ and rotational speed of $\sim 10^6$ cm s^{-1} provides a reservoir of 10^{47} ergs, which could power the most energetic outflows observed. Acceleration to supersonic speeds is accomplished by the magnetic field embedded in the disk (parallel rotational and magnetic axes) and extending outward beyond the wind region to join the galactic field. The wind carries angular momentum and energy from the disk out to large distances. Our analysis treats the problem of magnetic braking and energy transport in a partially ionized (two-fluid) wind. The basic parameter which is shown to govern the flow is the coupling parameter $\beta = T_{n-i}/T_{\rm fl}$, the ratio of the characteristic neutral-ion collision time to flow time. A general analysis of angular momentum and energy transport is given, and the wind equation is solved along flux tubes in the strongly coupled ($\beta \ll 1$) limit. The centrifugally driven wind forms when an embedded protostar begins to ionize the disk core region. A disk envelope forms at the wind base at a pressure which adjusts to the wind requirements. Envelope heating may be maintained by magnetic flux loss from the dense core (which has a field $\sim 10^{-3}$ gauss) that is preferentially along the rotation axis for flattened disks. The structure of the field at the disk core surface is derived. The observational implications are discussed; in particular, we emphasize that such molecular disks with double profiles should be observed.

Subject headings: hydromagnetics — interstellar: molecules — stars: pre–main-sequence

I. INTRODUCTION

Observations of $J = 2$–1 and $J = 1$–0 transitions in ^{12}CO and ^{13}CO in dense molecular clouds have revealed the presence of high-speed bipolar molecular gas outflows that are associated with embedded regions of star formation. Snell, Loren, and Plambeck (1980) found lobes of CO emission separating at speeds of order 15 km s^{-1} in the cloud L1551. These lobes are symmetrically placed about the infrared source on a scale of ~ 0.5 pc. Downes *et al.* (1981) find outflow speeds of 18 km s^{-1} in the KL region of Orion, on a scale of 2×10^{17} cm, where the flow rams into ambient gas of density $n_n \approx 10^5$–10^6 cm^{-3}. They conjecture that the central infrared source IRC 2 (a young, massive star) is responsible for energizing an outflow of 10^{-4}–$10^{-3}\ M_\odot$ yr^{-1}, over a period of 10^3–10^4 yr. Lada and Harvey (1981) have grouped together the most energetic outflows yet seen (in the clouds GL 490, Orion, Cep A, and L1551) as a class characterized by the following four properties: (1) large CO velocity dispersions ($\Delta v \geq 30$ km s^{-1}); (2) short dynamical time scales ($10^3 \leq T_{\rm fl} \leq 10^4$ yr); (3) anisotropic bipolar outflow centered about an embedded infrared source; and (4) large kinetic energies (10^{45}–10^{48} ergs). They have concluded that if these flows have been steady over these time scales, then radiatively driven winds are insufficient (by perhaps a factor of 10^2) to explain the highest energy outflows. Kwan and Scoville (1976) and Scoville (1981) pointed out such a discrepancy in Orion. Snell and Edwards (1981) have noted that central young stars with vastly different infrared luminosities seem to be able to power similar mass loss events in the course of their pre–main sequence evolution. In view of this analysis, Lada and Harvey suggested that other mechanisms, perhaps involving rotating magnetic fields near young stars, ought to be investigated. Königl (1982) has developed a unifying model which links the existence of high proper-motion Herbig-Haro objects (aligned with the outflow; see Snell and Edwards), separating broad-wing CO emission-line lobes, and cometary and bipolar nebulae, through one outflow mechanism. The outflow source is a spherically symmetric stellar wind which expands into an anisotropic external density distribution (due to either rotation or magnetic field), ultimately forming a de Laval nozzle

© American Astronomical Society • Provided by the NASA Astrophysics Data System

1983ApJ...274..677P

which channels the flow into oppositely directed supersonic jets. This idea explains the lower energy flows and, if the highest energy outflows are shown to have not necessarily been steady over 10^4 yr, could explain these as well.

The purpose of this work is to investigate the alternative possibility that the prime energy supply for the flows is from rotation and that the observed bipolar flows are centrifugally driven magnetic winds in which the rotational energy of a central dense region is carried off as an ordered supersonic outflow. The central point here is that this process is a "quiet" way of running an energetic wind, as the constraints of Lada and Harvey seem to require. Hartmann and MacGregor (1982) have proposed that such a mechanism operates in Orion where a rapidly rotating protostar of mass 10 $M_\odot$ and scale 10^{14} cm is suggested to be the central energy source. Their analysis considers a spherically symmetric wind from such a body in the limit that the ionization fraction is high enough that a one-fluid model for the flow can be adopted (the "strongly coupled" limit in our terminology).

In this work, we consider the general problem of wind outflows in two-fluid (partially ionized) magnetic clouds and treat the problem of magnetic field structure by specifying how flux tubes diverge in the cloud. The magnetic slingshot effect accelerates gas from the top of an envelope surrounding a dense disk core, out along open field lines to supersonic speed. Two sources of rotational energy are available here. The first could be that of a massive protostar itself. While this might be relevant for lower energy outflows, the very highest energy sources would require that a 3 $M_\odot$ star, say, rotate at close to breakup speeds. We propose instead that a dense interstellar molecular disk (in which the protostar is embedded) is the energy supply. A disk of mass ~ 100 $M_\odot$ would require a characteristic rotational speed of $\sim 10^6$ cm s^{-1} to power the most energetic winds.

It is shown later on that the outflow requires a rather oblate disk, on scales $\sim 10^{16}$ cm. A mass loss rate of 10^{-4} $M_\odot$ yr^{-1} in the resulting wind carries off the angular momentum in this rotational reservoir. The symmetry axis is that of the disk, which is assumed to be aligned with the axis of the initially forming star, and hence with the infrared source axis. The magnetic field is taken to be that of a bundle of galactic field lines (ordered on scales ≥ 10 pc) along which gas has contracted to finally form an oblate magnetically and rotationally supported disk (see Mouschovias 1976). The rotation axis of the disk is expected to be parallel to the magnetic axis. Vrba, Strom, and Strom (1976) have made polarization maps of several dark clouds in which star formation is occurring and conclude that the magnetic field is often aligned with optical streamers that project out from the formation region.

We will argue (in § V) that the disk envelope pressure is maintained by constant ambipolar magnetic flux loss from the dense underlying disk core. In the presence of an ionizing protostellar region embedded in the disk core, flux loss can accelerate as it moves up the rotation axes (in a flattened disk) and "slams" into the envelope, heating and/or accelerating this gas and thereby feeding the centrifugal drive. Flux loss on slow enough time scales allows disk core contraction whose associated energy release then is the ultimate power source for the disk envelope. In this scheme, centrifugally driven wind and disk core magnetic flux loss are intimately related.

The idea that centrifugally driven winds carry off angular momentum and energy from an underlying disk has been investigated by Blandford and Payne (1982) as a possible explanation of radio jets seen in active galactic nuclei. Our work envisions a similar process to be operative in the molecular cloud context, with some important differences. In molecular clouds, where the ionization fraction is tiny ($x \leq 10^{-7}$), the efficiency of magnetic braking depends critically on the value of x. Braking of the disk will occur only if the neutral gas is strongly coupled to the field by neutral-ion collisions. If a given neutral collides with ions on a time scale T_{n-i}, and the flow time scale is $T_{\rm fl}$, then the neutrals are only strongly coupled to the field when $\beta = T_{n-i}/T_{\rm fl} \ll 1$. The neutrals, ions, and field move closely together, and a steady-state wind outflow is possible. When the flows are weakly coupled ($\beta \gg 1$), the field (and ions) slips quite drastically with respect to the neutrals, and little angular momentum can flow. If the flux is not anchored in a central region (by higher than critical ionization fraction there), then magnetic flux will slip out of the gas, and the whole flow is highly time dependent. Our analysis will show that β is the basic coupling and control parameter in this problem. Hartmann and MacGregor have discussed the importance of this parameter in their work and correctly point out that, when $\beta \ll 1$, a one-fluid approach is entirely self-consistent.

Our analysis focuses on the structure and energy transport of this MHD wind as it moves out from the envelope of a dense molecular disk into the surrounding molecular cloud. The disk is taken to be in a state of near "magneto-centrifugo-gravitational" balance. Because of ambipolar diffusion (see Mouschovias 1981 for a review), some small rate of flux loss occurs, so a gentle disk contraction takes place. The mass of the disk must be less than the critical mass that can be held up by the embedded magnetic flux; $M \leq M_c$, where $M_c = \mathcal{F}/(G\pi)^{1/2}$ (see Mestel and Paris 1979). Mestel and Paris investigated the magnetic braking of a spherical cloud in the state described. They regarded the flux loss rate as a parameter that could be varied to fit the problem at hand. In this analysis we focus on axisymmetric conditions and suggest that a strong centrifugally driven wind will occur in the circumstance that a protostar turns on in the disk. When a protostar turns on, it is possible for it to provide sufficient ionization for the field to "grab" gas in a disk envelope and accelerate it away relatively efficiently, thereby removing angular momentum (and energy) from the disk. In addition, magnetic flux loss under such conditions may be sufficient to maintain the envelope pressure by some sort

© American Astronomical Society • Provided by the NASA Astrophysics Data System

1983ApJ...274..677P

of heating or acceleration process. This is a purely magnetic effect in a partially ionized medium wherein ambipolar diffusion always occurs.

In summary, the intent of this paper is twofold: the first is to examine the general properties of a cold MHD wind in a molecular cloud (§§ III and IV); the second, to analyze the conditions that must exist in the dense rotating molecular disk which is the "centrifuge" (§ V). The assumptions and equations behind the two-fluid approach used are stated in § II. We then focus on how angular momentum (§ III) and energy (§ IV) are transported away from the rotating interstellar disk by a cold centrifugally driven, MHD wind. The analysis of disk structure (§ V) concerns the formation of a disk envelope and the geometry of the disk magnetic field ("centrifuge arms"). A qualitative discussion of the results and observational implications is given in § VI, and the reader may find it helpful to read this before going on to § II.

II. ASSUMPTIONS AND BASIC EQUATIONS

It will be assumed throughout this paper that the flows are *steady* ($\partial/\partial t = 0$) and *axisymmetric* ($\partial/\partial\phi = 0$). As long as the gas has less than the critical mass for the magnetic flux it contains ($M < M_c$), only slow gravitational contraction can occur in the disk region. Also, the implication is that we are in a strong coupling regime where flux leakage is very small. Under these conditions, the steady-state assumption ought to be good, and the analysis can then focus on the spatial structure of the molecular wind. The assumption of axisymmetry picks out as the rotation axis that of a dense molecular disk, inside which protostars are forming. The third basic assumption is that *the flows are all laminar* so that turbulent transport processes will not be investigated. This assumption may be more difficult to justify if the CO line widths of O (km s^{-1}) arise by turbulent broadening. The main effect this has in an MHD wind theory is to replace the ohmic dissipation with turbulent diffusivity η_T. The "frozen-in" field picture, quite apart from any consideration of ambipolar diffusion, would not then be so good. Finally, it is assumed that there is one dominant neutral species (H_2) and a dominant ion species characterizing the partially ionized gas, so that *a two-fluid picture ignoring chemical reactions* will be adopted for greater simplicity. We will say a little more about cloud chemistry in what follows.

a) *Continuity*

The continuity equation for the neutrals is

$$\nabla\cdot(\rho_n \boldsymbol{v}_n) = 0, \tag{1}$$

where ρ_n is the neutral gas density and $\boldsymbol{v}_n$ its velocity. The subscript n will denote neutral gas quantities and i ion gas quantities. The ions obey

$$\nabla\cdot(\rho_i \boldsymbol{v}_i) = \begin{cases} 0 & \text{(slow recombination)} \quad (2a) \\ S_i & \text{(fast recombination)}, \quad (2b) \end{cases}$$

where ρ_i and $\boldsymbol{v}_i$ are the ion density and velocity and S_i is a source function for the ions.

The meaning of the two limits in equation (2) is as follows: if the advective time scale $T_{\rm fl}$ is much shorter than the time scale characteristic for ion recombination $T_{\rm recomb}$, then the number of ions in some blob of fluid remains constant as it moves along. This is the "*slow*" *recombination rate* limit (2a), and is the limit which will be adopted throughout the paper. Conversely, if recombination times are such that $T_{\rm recomb} \ll T_{\rm fl}$, then a source term S_i must appear, and (2b) holds. This is the "fast" recombination rate, and some basic features of this limit are given in the Appendix. Mouschovias and Paleologou (1981) have studied time-dependent, ambipolar diffusion problems in slab geometry in these two limits (which they call "slow" and "instantaneous," respectively). The slow recombination limit is of interest not just because of mathematical simplicity, but because the most vigorous outflows (such as the highly supersonic molecular gas outflows observed) will have flow time scales short compared to the recombination time scale.

To make this last point clear, we digress into a brief discussion of cloud chemistry, taken from Oppenheimer and Dalgarno (1974) and Thaddeus (1977). Low-energy cosmic rays ionize H_2, which quickly results in the formation of H_3^+ by $H_2^+ + H_2 \rightarrow H_3^+ + H$. Now H_3^+ is a fairly stable, long-lived ion that can lead to the formation of HCO^+ by the reaction $H_3^+ + CO \rightarrow HCO^+ + H_2$. HCO^+ is one of the most abundant interstellar molecules. It may be destroyed by dissociative recombination ($HCO^+ + e \rightarrow CO + H$), with rate coefficients typically $\sim 10^{-6}$ cm^3 s^{-1}. However, the important point is that HCO^+ may also undergo charge transfer to heavy metals (Ca, Mg, Na, etc.), producing singly charged heavy metal ions (Ca^+, Mg^+, Na^+, etc). These are chemically inert but can radiatively recombine with free electrons ($Ca^+ + e \rightarrow Ca^+ + h\nu$) or can recombine on negatively charged grains. It is the recombination step that is the slowest in the chain, and the relevant time scale here is the one which decides whether an ion source term S_i is

© American Astronomical Society • Provided by the NASA Astrophysics Data System

1983ApJ...274..677P

important. The recombination rates are for radiative recombination:

$$t^{-1}_{\text{rad.recomb.}} \approx 10^{-6}\left(\frac{\alpha_r}{10^{-11}\ \text{cm}^3\ \text{s}^{-1}}\right)\left(\frac{x}{3\times 10^{-7}}\right)\left(\frac{n_n}{10^5\ \text{cm}^{-3}}\right)\ \text{yr}^{-1}, \tag{3}$$

while for recombination on grains (Elmegreen 1979),

$$t^{-1}_{\text{grain}} \approx 10^{-6}\left[\left(\frac{T}{10\ \text{K}}\right)^{1/2}\left(\frac{a}{10^{-5}\ \text{cm}}\right)^2\left(\frac{m_{\text{ion}}}{40\ \text{amu}}\right)^{-1/2}\right]\left(\frac{D}{10^{-12}}\right)\left(\frac{n_n}{10^5\ \text{cm}^{-3}}\right)\ \text{yr}^{-1}, \tag{4}$$

where $D \equiv n_{\text{grain}}/n_n$ and a is the grain size. The point is that as x becomes smaller than $\sim 10^{-8}$ in cold clouds, the main mechanism of metallic ion recombination goes over from radiative to grain domination (Elmegreen 1979).

For our purposes it is sufficient to note that for flow times characterizing the supersonic molecular gas outflow, $T_{\text{fl}} \leq 10^4$ yr, the slow recombination time limit is an excellent approximation. The steady state is maintained by a central source of ions, assumed to rise in the star-forming regions of the disk.

b) *Equations of Motion*

The equations of motion for the neutrals and ions are, respectively,

$$\rho_n \boldsymbol{v}_n \cdot \nabla \boldsymbol{v}_n = -\nabla p_n - \rho_n \nabla \Phi + \boldsymbol{F}(-\boldsymbol{v}), \tag{5}$$

$$\rho_i \boldsymbol{v}_i \cdot \nabla \boldsymbol{v}_i = -\nabla p_i - \rho_i \nabla \Phi + \frac{\boldsymbol{j}\times\boldsymbol{b}}{c} + \boldsymbol{F}(\boldsymbol{v}), \tag{6}$$

where again, $j = n, i$ are neutral and ion labels, p_j is the pressure, ρ_j the density, Φ the gravitational potential, and $\boldsymbol{F}$ the friction force between ions and neutrals due to ion-neutral collisions. This force has the form (see Mestel and Spitzer 1956)

$$\boldsymbol{F}(\boldsymbol{v}) = n_{in}\rho_i\rho_n\boldsymbol{v}, \qquad \boldsymbol{v} \equiv \boldsymbol{v}_n - \boldsymbol{v}_i, \tag{7}$$

where $\boldsymbol{v}$ is the ion-neutral drift velocity and $\rho_i\eta_{in}$ is the neutral-ion collision frequency. Here η_{in} is related to the Langevin collision rate constant as

$$(m_n + m_i)\eta_{in} = \langle \sigma u \rangle_{in} \approx 10^{-9}\ \text{cm}^3\ \text{s}^{-1}, \tag{8}$$

where u is of order the sound speed in the gas. The term $\boldsymbol{j}\times\boldsymbol{b}/c$ in equation (6) is the Lorentz force which appears directly in the ion equation but is coupled, through $\boldsymbol{F}(\boldsymbol{v})$, to the neutrals. Here $\boldsymbol{j}$ is the current and $\boldsymbol{b}$ is the magnetic field.

c) *Magnetic Field*

The steady-state Maxwell equations are

$$\nabla \times \boldsymbol{E} = 0; \tag{9a}$$

$$\nabla \times \boldsymbol{b} = \frac{4\pi}{c}\boldsymbol{j}, \qquad \nabla \cdot \boldsymbol{b} = 0. \tag{9b}$$

The relation between the current $\boldsymbol{j}$ and the electric field $\boldsymbol{E}$ is established through Ohm's law, which for a partially ionized gas is

$$\boldsymbol{j}/\sigma = \boldsymbol{E} + \boldsymbol{v}_i \times \boldsymbol{b}/c - \boldsymbol{j}\times\boldsymbol{b}/n_n ec, \tag{10}$$

where σ is the conductivity (due to the electrons) and n_n is the neutral number density. The last term is known as the "Hall" term (Krall and Trivelpiece 1973) and is important in laboratory MHD power generators which employ

© American Astronomical Society • Provided by the NASA Astrophysics Data System

1983ApJ...274..677P

partially ionized gases. It is completely negligible in the astrophysical context ($L \approx 10^{-1}$ pc, $b \approx 10^{-4}$ gauss, $n_n \approx 10^6$ cm^{-3}). As long as the flow remains reasonably laminar, the magnetic Reynolds number (based on the Spitzer diffusivity $\eta = c^2/4\pi\sigma$) is enormous. Hence, the electric field is $\boldsymbol{E} = -\boldsymbol{v}_i \times \boldsymbol{b}/c$, and the steady Maxwell equations become

$$\nabla \times (\boldsymbol{v}_i \times \boldsymbol{b}) = 0. \tag{11}$$

d) *Gravitation and Pressure*

The Poisson equation for a weakly ionized gas ($x \ll 1$) is

$$\nabla^2 \Phi = 4\pi G \rho_n. \tag{12}$$

The pressure is related to density in polytropic fashion

$$p_j \propto \rho_j^{\gamma} \tag{13}$$

for each component j, with the same adiabatic index γ.

The strategy adopted throughout is to work along field lines when possible. This is clearly useful in strongly coupled flows. The assumption of axisymmetry imposes a very important relation between $\boldsymbol{v}_i$ and $\boldsymbol{b}$ when equation (11) holds. To facilitate the analysis, all vector fields are decomposed into poloidal and toroidal components $\boldsymbol{A} = \boldsymbol{A}_p + \boldsymbol{A}_\phi$ (i.e., $\boldsymbol{v}_n = \boldsymbol{v}_{p,n} + \boldsymbol{v}_{\phi,n}$, etc; cylindrical coordinates will be used). With this decomposition, it is easily shown (see Chandrasekhar 1956 and Mestel 1961) that in axisymmetric conditions, equation (11) admits the general integrals

$$\boldsymbol{v}_{p,i} = \kappa \boldsymbol{b}_p, \tag{14}$$

$$v_{\phi,i} = \alpha r + \kappa b_\phi, \tag{15}$$

where κ is some scalar function of the coordinates and α is constant along each field line and can be regarded as the angular frequency of that field line.

In the slow recombination limit [$\nabla \cdot (\rho_i \boldsymbol{v}_i) = 0$] equation (14) is used to show that also

$$\kappa \rho_i = \text{const. on a field line.} \tag{16}$$

The results (14)–(16) have the same form for a completely ionized gas for which $\nabla \cdot (\rho \boldsymbol{v}) = 0$, and as discussed by Mestel (1968), lead to the presence of a third integral in the problem. In the completely ionized gas, $\boldsymbol{F} = 0$, and the ϕ component of equation (6) (angular momentum conservation) leads to (using eqs. [14] and [16])

$$\boldsymbol{b} \cdot \nabla (L) = 0, \tag{17}$$

$$L \equiv r v_\phi - \frac{r b_\phi}{4\pi\kappa\rho} = \text{const. on a field line,} \tag{18}$$

where it is understood that the gas is totally ionized and the indices have been dropped. The constant L along a field line is the total specific angular momentum. It is comprised of a material contribution (rv_ϕ) and a contribution arising from the magnetic field itself.

The presence of friction $\boldsymbol{F}$ in a partially ionized gas complicates the issue of angular momentum transport along field lines, but the next section shows that things work nicely in a strong coupling limit.

III. ANGULAR MOMENTUM TRANSPORT

The question of how angular momentum is transported in a partially ionized gas with magnetic field is a complicated one because all of the neutrals, ions, and field will contribute. The crucial point is how strongly these flows are coupled with one another's motions (see Hartmann and MacGregor 1982).

The key parameter is the coupling β, discussed in the introduction. If a given neutral atom collides many times with ions in a time scale characteristic of the flow, then $\beta \ll 1$ and the constituents move together. We show how various regimes for angular momentum and energy flow are demarcated by β.

© American Astronomical Society • Provided by the NASA Astrophysics Data System

1983ApJ...274..677P

From equation (7), β is

$$\beta \equiv T_{n-i}/T_{\rm fl} = v_{\rm fl}/\rho_i \eta_{in} L_{\rm fl}. \tag{19}$$

When x is as low as 10^{-7} and $n_n \approx 10^6$ cm^{-3}, the neutral-ion collision time scale is of order 10^3 yr, so that clouds with flow time scales of 10^4 yr are strongly coupled. In the weakly coupled regime ambipolar diffusive effects predominate. If the flux is not anchored in some central, sufficiently ionized core, the magnetic field will rapidly readjust so that a highly time variable flow may arise.

To proceed, the angular momentum equations for the ions and neutrals will be considered. The third relation between the three toroidal fields ($v_{\phi i}$, $v_{\phi n}$, and $\boldsymbol{b}_\phi$) is provided by equation (15), which arises from the induction equation.

The angular momentum equation for the ion gas (ϕ component of eq. [6]) is

$$\rho_i \boldsymbol{v}_{p,i} \cdot \nabla (r v_{\phi,i}) - \boldsymbol{b}_p \cdot \nabla \left(\frac{r b_\phi}{4\pi} \right) = r F_\phi(\boldsymbol{v}). \tag{20}$$

This shows that the amount of angular momentum that is carried by the streaming ion gas is the difference between the magnetic and frictional torques acting on each volume of gas. In the slow recombination limit, equation (20) may be written

$$\rho_i \boldsymbol{v}_{p,i} \cdot \nabla (L) = r F_\phi(\boldsymbol{v}), \tag{21}$$

where L is the combination of specific ion and field contributions to the angular momentum (given in eq. [18]). Recall that L is constant along field lines in the completely ionized gas ($\boldsymbol{F} = 0$).

The angular momentum equation for the neutrals is (ϕ component of eq. [5])

$$\rho_n \boldsymbol{v}_{p,n} \cdot \nabla (r v_{\phi,n}) = - r F_\phi(\boldsymbol{v}), \tag{22}$$

which shows that the amount of angular momentum carried by the streaming neutral gas depends on the frictional torque acting on each volume. Note the action of this torque is in a sense opposite to that in the ion gas.

Before proceeding to angular momentum transport in the total gas, we shall examine equation (22) more closely. Substitution of the form (7) for F_ϕ into equation (22) gives

$$- v_\phi \approx \beta v_{\phi,n}, \tag{23}$$

where

$$\beta \equiv \frac{v_{p,n}}{x \rho_n \eta_{in} s} \approx \frac{10^{-1}}{(x/10^{-7})} \frac{(v_{p,n}/10^6 \text{ cm s}^{-1})}{(n_n/10^6 \text{ cm}^{-3})(s/10^{17} \text{ cm})} \tag{24}$$

is the ratio of ion-neutral collision time scale to ion flow time scale, and s is a scale characteristic of $r v_{\phi,n}$ as it varies in the direction of $\boldsymbol{v}_{p,n}$.

There are two points of importance here. For $\beta \ll 1$ (i.e., $x \geq 10^{-8}$), the toroidal drift v_ϕ is small compared to $v_{\phi,n}$, and the ions and neutrals (and therefore field) are "strongly coupled." For $x \leq 10^{-8}$, however, the toroidal drift becomes large relative to $v_{\phi,n}$, and the fluids are "weakly coupled." (Notice that for $n_n \approx 10$ cm^{-3}, say, weak coupling sets in when $x \leq 10^{-2}$.) Thus, the coupling parameter spans the range $10^{-1} \leq \beta \leq 10$ for the interesting range of ionization fractions ($10^{-7} \leq x \leq 10^{-9}$) that may occur in the densest molecular clouds.

The second point to make about equation (23) concerns the relative signs of the flows. A stable distribution of neutral angular momentum requires $\partial / \partial r (r v_{\phi,n}) > 0$. In a neutral accretion regime, therefore, where $v_{p,n} < 0$,

$$v_{\phi,i} - v_{\phi,n} < 0,$$

so that the ions always just lag the neutrals. Conversely, in the outflow regime, where $v_{p,n} > 0$, the neutrals would lag the ions.

© American Astronomical Society • Provided by the NASA Astrophysics Data System

1983ApJ...274..677P

Addition of equations (21) and (22) gives the angular momentum equation for the entire gas, viz.,

$$\nabla\cdot\left[\rho_i \mathbf{v}_{p,i}\left(rv_{\phi,i}-\frac{rb_\phi}{4\pi\kappa\rho_i}\right)+\rho_n \mathbf{v}_{p,n}(rv_{\phi,n})\right]=0. \tag{25}$$

In all generality, the neutral and ion streamlines are different, so that without any approximation it is impossible to single out a characteristic surface in the partially ionized gas, along which some total specific angular momentum remains constant. The problem simplifies greatly in the regimes discussed, however.

The ratio of neutral to ion angular momentum flux (Γ) is $\Gamma = v_{\phi,n}v_{pn}/xv_{\phi,i}v_{pi}$. This ratio is evaluated with equation (23) to give

$$\Gamma \approx (\beta x)^{-1}\left(\frac{v_\phi}{v_{\phi,i}}\right)\left(\frac{v_{p,n}}{v_{p,i}}\right). \tag{26}$$

Two cases may now arise. If the flow is strongly coupled, then $v_\phi/v_{\phi,i}\approx\beta$, and hence $\Gamma\approx x^{-1}$. Therefore, in strongly coupled flows, the neutrals carry the material part of the angular momentum flux as long as $x=\rho_i/\rho_n<1$. The second case in equation (26) is that for weak coupling, where now $v_\phi\approx v_{\phi,i}$, and thus $\Gamma\approx(\beta x)^{-1}$. As long as $\beta x<1$, then, the neutrals carry the angular momentum here as well. However, note that if $x>\beta^{-1}$, the ions would carry the material part of the angular momentum flux.

To return to the main point again, the strongly coupled flows will have angular momentum carried by neutrals and field when $x<1$. The angular momentum equation is then

$$\nabla\cdot\left[\rho_n \mathbf{v}_{p,n}(rv_{\phi,n})-\rho_n \mathbf{v}_{p,i}\left(\frac{rb_\phi}{4\pi\kappa\rho_n}\right)\right]=0, \tag{27}$$

and the question becomes how different are $v_{p,n}$ and $v_{p,i}$? If

$$v_p/v_{p,n}\ll 1, \tag{28}$$

then $v_{p,i}\approx v_{p,n}$, and the poloidal ion and neutral flows are locked together. If the force balance for the ion flow is considered in the cloud, then inside the position of critical points in the flow the friction and Lorentz forces nearly balance (ion pressure and gravity negligible), as discussed in Spitzer (1978). Hence, this balance gives

$$v_p/v_{p,n}\approx\beta\frac{v_{A,n}^2}{v_{p,n}^2}. \tag{29}$$

In the limit (28), the condition for strong coupling of the poloidal flows is

$$\beta\ll\frac{v_{p,n}^2}{v_{A,n}^2}<1, \tag{30}$$

where $v_{A,n}^2=b_p^2/4\pi\rho_n$ is the Alfvén speed based on the neutral gas density, and we are inside the region where any critical points reside.

The angular momentum equation in the high density, strongly coupled regime is then

$$rv_{\phi,n}-\frac{rb_\phi}{4\pi\kappa\rho_n}=\text{const. on a field line}\equiv\tilde{L}. \tag{31}$$

Simultaneous solution of equations (31), (15), and (23) gives

$$v_{\phi,n}=\frac{1}{r}\frac{\tilde{L}-(\alpha r^2/4\pi\kappa^2\rho_n)}{1-(1+\beta)/4\pi\kappa^2\rho_n}, \tag{32}$$

$$b_\phi=\frac{1}{\kappa r}\frac{(1+\beta)\tilde{L}-\alpha r^2}{1-(1+\beta)/4\pi\kappa^2\rho_n}, \tag{33}$$

© American Astronomical Society • Provided by the NASA Astrophysics Data System

1983ApJ...274..677P

and

$$v_{\phi,i} = (1+\beta)v_{\phi,n}.$$

The Alfvénic point $r_{A,n}$ occurs when $4\pi\kappa^2\rho_n = 1+\beta$, or

$$\frac{b_p^2}{4\pi} = (1+\beta)^{-1}\rho_n v_{p,n}^2, \tag{34}$$

which is closer in to the origin. The constant $\tilde{L}$ is then

$$\tilde{L} = \alpha r_{A,n}^2 (1+\beta)_{r_{A,n}}^{-1}, \tag{35}$$

which shows that because the lever arm has moved in by a factor $(1+\beta)^{-1/2} r_{A,n}$ from the "naive" guess, less angular momentum can be transported out.

These results show that the coupling β is the physical parameter under which the important properties of flows in molecular clouds can be organized. Qualitatively new effects appear in equations (31)–(35), even though they are small in magnitude in the strong coupling limit. Because $\beta = (-v_\phi/v_{\phi,n})$, it is seen in equation (35) that the efficiency of angular momentum transport is affected by the toroidal slip of field lines at the Alfvénic point relative to the neutral fluid. As the coupling becomes weaker, this slip will increase to the point that L decreases dramatically. In the analogy of the magnetic field behaving like a "wire" along which gas streams (Henricksen and Rayburn 1971), the slip of the material relative to the field line will reduce angular momentum transport efficiency. Note that the neutrals *lag* the field for outflow and the ions sit with the field lines.

The fact that the field line slip depends upon x at the Alfvénic point shows that whatever controls the ionization fraction at this point will control angular momentum transport in the wind, and hence the evolution of whatever is driving the wind in the first place. Two possibilities arise: (i) x_{r_A} is controlled by external ionizing agents; and (ii) the wind itself regulates x_{r_A}. The important point about the first possibility is that the formation of an OB star, as an example, will enhance braking processes in the vicinity, allowing more OB stars to form in the region (see § IV). The possibility of self-regulation (ii) would not make environmental effects so important. This is discussed in § VI. The mass loss rate in the outflow in the high density, strongly coupled regime is

$$\dot{M}_{\rm wind} = \int_{\mathscr{A}} \rho_n \boldsymbol{v}_{p,n} \cdot d\boldsymbol{A} \approx 4\pi (\rho_n v_{p,n})_{R_{A,n}} R_{A,n}^2 \Omega, \tag{36}$$

where $\mathscr{A}$ is the area of the Alfvénic surface and Ω is the solid angle it subtends. In order to account for an outflow of $\dot{M}_{\rm wind} \approx 10^{-4}\ M_\odot\ {\rm yr}^{-1}$ (take $r_{A,n} \approx R_{A,n} \sin\Theta$ for flows of opening angle 2Θ), we find that for vigorous outflows,

$$\dot{M}_{\rm wind} \approx 10^{-4}\ M_\odot\ {\rm yr}^{-1} \left(n_n/10^5\ {\rm cm}^{-3}\right)\left(v_{p,n}/10^7\ {\rm cm\ s}^{-1}\right)\left(\Omega/10^{-1}\right)\left(R_{A,n}/10^{17}\ {\rm cm}\right)^2. \tag{37}$$

It is evident that the Alfvénic radius should lay at about $R_{A,n} \approx 10^{17}$ cm (note that smaller opening angles will give $\dot{M} \approx 10^{-5}\ M_\odot\ {\rm yr}^{-1}$, say). An accurate estimate of ρ_n and $v_{p,n}$ comes from the analysis of the poloidal flow energy equation, which is taken up in the next section.

The angular momentum flux carried by this wind is

$$\dot{L}_{\rm wind} = \int_{\mathscr{A}} L\rho_n \boldsymbol{v}_{p,n} \cdot d\boldsymbol{A} \approx \dot{M}_{\rm wind} \alpha R_{A,n}^2 (1-\beta)_{R_{A,n}}. \tag{38}$$

This flux arises from the magnetic braking of some object on much smaller scales than 10^{17} cm. We suggest this condensed object is a flattened, dense molecular disk, which is threaded by the open field lines. The angular frequency of such a massive disk is changing at a rate α, on a time scale very slow compared to the wind time scale. Therefore, the angular momentum flux lost to the disk is of order

$$\dot{L}_{\rm disk} \approx \dot{\alpha} M_{\rm disk} R_{\rm disk}^2, \tag{39}$$

© American Astronomical Society • Provided by the NASA Astrophysics Data System

1983ApJ...274..677P

assuming negligible mass loss and contraction of the disk (to zeroth order only!). It follows that if $\dot{L}_{\rm disk} \approx \dot{L}_{\rm wind}$, then

$$\frac{M_{\rm disk}}{M_{\rm wind}} \approx \frac{R_{{\rm A},n}^2}{R_{\rm disk}^2}(1-\beta)_{R_{{\rm A},n}}. \tag{40}$$

For $M_{\rm wind} \approx 1\ M_\odot$ then, and $R_{\rm A} \approx 10^{17}$ cm, it follows that if $R_{\rm disk} \approx 10^{16}$ cm, then $M_{\rm disk} \approx 100(1-\beta)\ M_\odot$. It is readily seen that the factor $1-\beta$ is important for setting the exact mass of the dense molecular disk and therefore has some effect on star formation efficiency inside the disk. In this picture, the interpretation of the massive observed bipolar outflows as centrifugally driven demands the existence of a fairly massive molecular disk at the core.

The result (40) bears a very direct relation to the work of Mouschovias and Paleologou (1980), in which the magnetic braking of a disk of density $\rho_{\rm cl}$, embedded in an external medium of density $\rho_{\rm ext}$ was studied in the case where the magnetic field and angular momentum axes are aligned. This work pointed out that significant cloud braking occurs when hydromagnetic waves propagating away from the cloud set into rotational motion an amount of external matter with moment of inertia equal to that of the cloud,

$$z_l \rho_{\rm ext} = z_{\rm cl} \rho_{\rm cl}, \tag{41}$$

for the case $\rho_{\rm cl} \gg \rho_{\rm ext}$, and where z_l and $z_{\rm cl}$ are the external scale height and half-thickness of the disk. Notice that this result is similar to ours (eq. [40]), where we identify the radius $R_{{\rm A},n}$ with z_l, except for the factor $(1-\xi/x)R_{{\rm A},n}$, which measures the field line slip at the Alfvénic radius. Thus, because the field lines are not rigidly connected to the external medium (because of the low ionization fraction), one has to go out further in order to have a balance of the moments of inertia of that material set into motion by the field and the moment of inertia of the disk.

This section may be concluded, then, by noting how important detailed information about x is. Although the ions do not carry angular momentum or energy in a regime such as would occur in bipolar outflows in molecular clouds, nevertheless the ionization fraction plays a central role. Thus, the condition for a steady, windlike outflow (eq. [31]), the specific angular momentum along a field line (eq. [35]), and the estimate for how much mass is carried out in a wind (eq. [40]) all depend upon x in a basic way. The key point is that the ionization fraction in such outflows in molecular clouds ought to be strongly correlated with the overall structure of the flow (steady, $\beta \ll 1$, or irregular, $\beta \gg 1$, etc).

VI. WIND ENERGETICS

In this section, the energetics of the cold MHD outflows is examined. It is imagined that the field lines thread a dense molecular disk, and the problem is to determine $v_{p,n}$ along the flux tubes.

The energy equations for the ions are, in the slow recombination time limit,

$$\nabla\cdot(\rho_i \boldsymbol{v}_{p,i}\mathscr{E}_i) = \boldsymbol{v}_i\cdot\boldsymbol{F}, \tag{42}$$

$$\nabla\cdot(\rho_n \boldsymbol{v}_{p,n}\mathscr{E}_n) = -\boldsymbol{v}_n\cdot\boldsymbol{F}, \tag{43}$$

where $\mathscr{E}_i$ and $\mathscr{E}_n$ are the total specific energy densities of the ion and neutral components (excluding friction):

$$\mathscr{E}_i \equiv c_s^2 \ln p_i + \Phi + \tfrac{1}{2}v_i^2 - \frac{r\alpha b_\phi}{4\pi\kappa\rho_i}, \tag{44}$$

$$\mathscr{E}_n \equiv c_s^2 \ln p_n + \Phi + \tfrac{1}{2}v_n^2. \tag{45}$$

The right-hand sides of equations (42) and (43) represent, respectively, the rate of work done by the friction upon the ion and neutral gases. The term $(-r\alpha b_\phi/4\pi\kappa\rho_i)\rho_i v_{p,i}$ is the Poynting flux and represents the entire contribution of the magnetic field.

The energy equation for the total gas is formed by summing equations (42) and (43). In the high density, strong coupling case, only the magnetic contribution from $\mathscr{E}_i$ is significant for the combined flow. The resulting expression is

$$\rho_n \boldsymbol{v}_{p,n}\cdot\nabla\left[c_s^2 \ln p_n + \Phi + \frac{v_{p,n}^2}{2} + \Omega_n\left(\frac{\Omega_n}{2} - \alpha\right)r^2\right] = \boldsymbol{v}\cdot\boldsymbol{F}, \tag{46}$$

where equation (36) is used to eliminate the dependence on b_ϕ. The last two terms on the left-hand side of equation

© American Astronomical Society • Provided by the NASA Astrophysics Data System

1983ApJ...274..677P

(46) represent the combined contribution of rotation and magnetic field. In the absence of friction, the equation is that used by Mestel (1968). The rate of heat production by friction is, in general, an interesting effect, because the gas would be kept "warm" as it moves out along the flux tube. We show that in the case of strong coupling, this heating represents a correction of $O(\beta)$ to the "frictionless" case and will not be important in controlling the nature of critical points in the flow.

Radiative cooling due to CO rotational transitions is an effect which further diminishes the right-hand side of equation (46), in principle. For the case of dense molecular gas, de Jong, Chu, and Dalgarno (1975) have estimated that for optically thick CO rotational transitions, the cooling rate is

$$\Lambda_{\rm rot} \approx \rho \left(\frac{10^{-5} \Delta v \, T_2^3}{n_6 r_{17}} \right) \text{ ergs s}^{-1} \text{ cm}^{-3}, \tag{47}$$

where Δv is the line width in km s^{-1} (see Hollenbach and McKee 1979, for a detailed analysis of this and other cooling processes). Comparison of equation (47) with $\boldsymbol{v} \cdot \boldsymbol{F}$ shows that as long as $v > 10^3$ cm s^{-1} and the flow is laminar, the frictional heating should dominate the CO cooling. This situation is quite different in a molecular shock, where CO cooling becomes very important (Hollenbach and McKee 1979).

The heating term in equation (46) is written as

$$\boldsymbol{v} \cdot \boldsymbol{F} = \frac{1}{\beta} \frac{\rho_n v_{p,n}}{s} \left(v_\phi^2 + v_p^2 \right),$$

and it is clear from equations (29) and (23) that it is of $O(\beta)$. To make this explicit, the rotational frequency Ω_n given by equation (32) is expanded in powers of β, so that to $O(\beta)$, the energy equation is

$$\rho_n \boldsymbol{v}_{p,n} \cdot \nabla \left[c_s^2 \ln p_n + \Phi + \frac{v_{p,n}^2}{2} + \Omega_n^{(0)} \left(\frac{\Omega_n^{(0)}}{2} - \alpha \right) r^2 \right]$$

$$= \beta \left\{ - \frac{\rho_n \boldsymbol{v}_{p,n}}{\beta} \cdot \nabla \left[\beta \Omega_n^{(1)} \left(\Omega_n^{(0)} - \alpha \right) r^2 \right] + \frac{\rho_n v_{p,n}}{s} \left(1 + \frac{v_{A,n}^4}{v_{\phi,n}^2 v_{p,n}^2} \right) \Omega_n^{(0)2} r^2 \right\} + O(\beta^2), \tag{48}$$

where $\Omega_n = \Omega_n^{(0)} + \beta \Omega_n^{(1)} + \cdots$.

The important features of the flow in strong coupling are determined to zeroth order in β by

$$\frac{d}{ds} \left[c_s^2 \ln p_n + \bar{\Phi} + \frac{v_{p,n}^2}{2} + \Omega_n^{(0)} \left(\frac{\Omega_n^{(0)}}{2} - \alpha \right) r^2 \right] = 0. \tag{49}$$

This is the same type of equation that has been studied by Weber and Davis (1967), Mestel (1968), and Goldreich and Julian (1970, henceforth GJ) in the context of stellar winds. The differences that arise are in the nature of the poloidal field b_p in the system under consideration.

To simplify the discussion, we will consider an isothermal gas (c_s = const) because frictional heating is a small effect in the strong coupling case. The density dependence in equation (49) is eliminated by using the condition that $\rho_n \kappa = \rho_n v_{p,n} / b_p$ = constant along field lines. The specific dependence upon b_p can be transferred into a dependence upon the cross-sectional area $\mathscr{A}$ of a flux tube as a function of s, as long as the analysis focuses on the flow along field lines. Then, because flux is conserved in the strong coupling limit,

$$\mathscr{F} \equiv \mathscr{A} b p = \text{const. on a flux tube.} \tag{50}$$

The factor ρ_n is eliminated by noting that the mass loss rate along a flux tube is now a constant; i.e.,

$$\rho_n v_{p,n} \mathscr{A} = \text{const. on a flux tube.} \tag{51}$$

In stellar wind problems with radial field lines, $\mathscr{A} \propto s^2$ (see GJ and Weber and Davis). The question of how field lines diverge in the case of a wind off a molecular disk is perhaps best answered observationally, but in any case, there

© American Astronomical Society • Provided by the NASA Astrophysics Data System

1983ApJ...274..677P

is no reason why the field should open purely radially. Hence, we will write

$$\mathscr{A} \propto s^{2k} \tag{52}$$

for the area of the flux tube, and note that $k=1$ for radial field lines. Thus, the main factor that affects the wind structure of strongly coupled flows is how the flux tubes diverge.

Holzer (1977) has written extensively on the effects of rapid flux tube divergence in the case of the solar wind (e.g., in coronal holes). In the case of rapid flux tube divergence, higher expansion speeds will occur at the coronal base so that smaller addition of energy above the coronal region is required to maintain the flow. Thus, in the stellar thermally driven wind, the sonic point occurs deeper in the stellar atmosphere.

To return to our problem, it is convenient to define the dimensionless variables

$$x \equiv s/r_0, \quad y \equiv r(s)/r_0, \quad u \equiv v_{p,n}/v_{p,n_0}, \quad c \equiv c_s/v_{p,n_0},$$

$$M_A^2 \equiv 4\pi\kappa^2\rho_n, \quad \psi \equiv \Phi/c_s^2, \quad \lambda \equiv \tilde{L}/\alpha r_0^2, \quad \sigma \equiv (\alpha r_0)^2/v_{p,n_0}^2, \tag{53}$$

where M_A^2 is the radial Alfvénic Mach number and r_0 is the cylindrical radius at which the field line is attached to the disk. Note that $M_A^2 = ux^{2k}$ in these variables. In addition, $\Omega_n^{(0)}$ takes the form

$$\Omega_n^{(0)} = \alpha\left(\frac{\lambda}{y^2}M_A^2 - 1\right)\Big/\left(M_A^2 - 1\right), \tag{54}$$

so that at the Alfvénic point, $M_A^2 = 1$, $\lambda/y^2 = 1$. In order to further simplify the analysis, it will be assumed that

$$y \propto x^t. \tag{55}$$

The substitution of equations (51)–(55) into the differential equation (49) gives

$$\frac{du}{dx} = \frac{u}{x}\left[\left(2k - x\frac{d\psi}{dx}\right)\left(M_A^2 - 1\right)^3 c^2 + \sigma y^2\left\{(\lambda u x^\nu - 1)\left[\left(M_A^2 + 1\right)\lambda u x^\nu - 3M_A^2 + 1\right] + 2M_A^4\left(\frac{\lambda}{y^2} - 1\right)^2\left(\frac{k}{t} - 1\right)\right\}\right]$$

$$\times\left\{\left(M_A^2 - 1\right)^3(u^2 - c^2) - \sigma\lambda^2 u^2 y^2 x^{2\nu}\left[1 - \frac{y^2}{\lambda}\right]^2\right\}^{-1}, \tag{56}$$

where $\nu = 2(k - t)$. It is seen immediately that the Alfvénic critical point is also a critical point of this equation for u. In the case that $k = t = 1$ ($\nu = 0$), the equation reduces to that of Weber and Davis (1967) and GJ.

To digress briefly, it is well known that in the radially extended wind ($\mathscr{A} \propto s^2$, for which $k = t = 1$), equation (56) shows two other critical points in addition to the Alfvénic point. These points are known as the sonic and magnetosonic critical points and correspond to points where the poloidal speed matches the poloidal propagation speed of sound waves and Alfvénic waves determined by the toroidal field. Normally the sonic point is close to the star and involves a balance between pressure and gravitational forces. The magnetosonic point lies beyond the Alfvenic point, and hence the gravity is generally negligible. In equation (56) the competition between gravitational drag and flux tube divergence is seen in the factor $2k - x\,d\Psi/dx$.

It is useful to define the parameter

$$d \equiv 2(k/t - 1) \tag{57}$$

which will be called the *divergence* of a flux tube. If $d < 0$, the cross-sectional area of the tube diverges less quickly than r^2, and the tube will be said to be "converging." The field lines in this case will tend to collimate along the rotation axis. Conversely, when $d > 0$, the flux tubes diverge faster than r^2, and will spread away from the axis. We now investigate the behavior of the critical points.

a) Magnetosonic Point

We will assume that this point occurs far enough away from the disk that the disk gravity is negligible and that the flow is highly supersonic as well ($u^2 \gg c^2$). The factor $(M_A^2 - 1)^3$ may be eliminated by the two conditions that the

© American Astronomical Society • Provided by the NASA Astrophysics Data System

1983ApJ...274..677P

denominator and numerator of equation (56) vanish at the critical point. A number of cases arise, and we divide them into two general categories: (i) $|d|u^2 \gg 2kc^2$, and (ii) $|d|u^2 \ll 2kc^2$.

i) $|d|u^2 \gg 2kc^2$

A quadratic equation for y^2 is found whose solution is

$$y_c^2 = \left[2\lambda + \frac{(\lambda U - 1)(3 - \lambda U)}{dU}\right]\left[\left[1 + \left\{1 - \frac{4(\lambda U - 1)(\lambda U + 1)d}{[2\lambda U d + (\lambda U - 1)(3 - \lambda U)]^2}\right\}^{1/2}\right]\right], \tag{58}$$

where $U = ux^{\nu}$ is a scaled poloidal speed. From the vanishing of the denominator of equation (56), and from equation (58), y_c and U_c can be found. A total of four subcases arise, which are now listed:
Case 1: $|d| \ll \lambda U$; $\lambda U \approx 1 + O(d)$:

$$y_c^2 \approx \lambda / (1 - \sigma\lambda^3 x_c^{2\nu});$$

$$(\lambda U_c)^{-1} \approx 1 - \frac{d}{2}\frac{\sigma\lambda^3 x_c^{2\nu}}{(1 - \sigma\lambda^3 x_c^{2\nu})}. \tag{59}$$

Case 2: $|d| \ll \lambda U$; $\lambda U \gg 1 + O(d)$:

$$y_c^2 \approx \frac{(\lambda U_c - 1)(3 - \lambda U_c)}{2dU_c} \gg 1;$$

$$U_c \approx (\sigma x_c^{2\nu})^{1/3}. \tag{60}$$

In the case that $\lambda U \gg d$, solutions only exist, provided that $d(\lambda U - 1) > 0$. The results are then
Case 3: $|d| \gg \lambda U$; $\lambda U \approx 1 + O(d^{-1})$:

$$y_c^2 \approx \lambda\left[1 + (\lambda U_c d)^{-1}\right];$$

$$\lambda U_c \approx (\sigma\lambda^3 x_c^{2\nu})^{1/2} d^{1/2}. \tag{61}$$

Case 4: $|d| \gg \lambda U$; $d > 0$; $\lambda U \gg 1 + O(d^{-1})$:

$$y_c^2 \approx \lambda(1 + d^{-1/2});$$

$$\lambda U_c \approx (\sigma\lambda^3 x_c^{2\nu})^{1/3} d^{-1/3}. \tag{62}$$

ii) $|d|u^2 \ll 2kc^2$

This is the case in which the divergence $d \approx 0$, and almost $\mathscr{A} \propto s^2$ is followed. The quadratic equation in this regime is identical to that written down by GJ, provided their poloidal speed is replaced with $U = ux^{\nu}$, the sound speed by $C^2 = kc^2 x^{2\nu}$, and their σ with $\Sigma = \sigma x^{2\nu}$. The relevant subcases are
Case 1: $\lambda U \approx 1 + O(C^2)$;

$$y_c^2 \approx \lambda / (1 - \sigma\lambda^3 x_c^{2\nu});$$

$$U_c^2 \approx \lambda^{-2} + C^2 \frac{\sigma\lambda^3 x_c^{2\nu}}{(1 - \sigma\lambda^3 x_c^{2\nu})}. \tag{63}$$

© American Astronomical Society • Provided by the NASA Astrophysics Data System

1983ApJ...274..677P

Case 2: $\lambda U \gg 1 + O(C^2)$:

$$y_c^2 \approx \frac{1}{2}\frac{U_c}{C^2}(\lambda U_c - 1)(3 - \lambda U_c) \gg 1;$$

$$U_c \approx \left(\sigma x_c^{2\nu}\right)^{1/3}. \tag{64}$$

The similarity between equations (59) and (63) arises because the limits $\lambda U \approx 1 + O(d)$ and $\lambda U \approx 1 + O(C^2)$ are taken. In the same way, equations (60) and (64) correspond. The results (61) and (62) do not have correspondence with cases in § IV*a*(ii), because always $C^2 \ll U^2$ at the magnetosonic point.

To interpret these results, note that from equations (33) and (51)–(53), the condition $u_c = \sigma^{1/3}$ is equivalent to

$$M_c^{-2} \equiv b_\phi^2/4\pi\rho_n v_{p,n}^2 \approx 1.$$

Note that $x_c \gg 1$ is required in order to find this. For this analysis the result for $y_c^2 \gg 1$ is that $u_c = \sigma^{1/3}/x_c^{\nu/3}$, so that the diverging (converging) flow is moving much slower (faster) at the magnetosonic point than the case for radial field lines, where $u_c = \sigma^{1/3}$. The other case that generally occurs is that $y_c^2 \approx \lambda$, which is to say that with $\lambda U_c \approx 1$, the sonic point and magnetosonic point lie fairly close to one another.

b) Sonic Point

The standard assumption is made that the sonic point occurs relatively close to the disk compared to the Alfvénic point. Then $M_A^2 \ll 1$, and the flow is very subAlfvénic. The vanishing of the denominator in equation (56) gives in this limit $u_s^2 \approx c^2/[1 + \sigma\lambda^3 x^{2\nu}(x^2/\lambda)] \approx c^2$. The vanishing of the numerator then gives (as long as k/t is not too large) the simple cubic

$$2kx - l + Klx^3 = 0,$$

where $l = GM_{\rm disk}/r_0c^2$ and $K = \alpha^2 r_0^3/GM_{\rm disk}$. This differs from the usual result only through the factor k, where for diverging flux tubes $k > 1$, and for converging, $k < 1$. Following GJ, the solution for $Kl^3 \ll 1$ is

$$x_s = l/2k, \tag{65}$$

which shows that for *diverging* flux tubes, the sonic point will occur deeper in toward the disk surface, as Holzer (1977) has discussed. For focused outflow ($k < 1$), the sonic point is farther out and closer to the Alfvenic point. In the limit that $Kl^3 \gg 1$, the result is

$$x_s = K^{-1/3}. \tag{66}$$

The limit $Kl^3 \ll 1$ corresponds to $\alpha r_0/c_s \ll 1$ (slow rotation). In this limit, if $c_s \approx 10^5$ cm s^{-1}, then the rotational speed is of order 10^4 cm s^{-1}, which is too slow for the most energetic outflows. Hence, highly oblate disks (for which supersonic rotational speed occurs) are governed by equation (66), or $r_s \approx (GM_{\rm disk}/\alpha^2)^{1/3} \approx 1.1 \times 10^{16}$ cm$(M/100\ M_\odot)^{1/3}(\alpha/10^{-10}\ {\rm s}^{-1})^{-2/3}$. Thus, disks rotating at speeds $v_{\phi,n} \approx 10^6$ cm s^{-1} will have the sonic point laying just above the disk envelope (taken to extend to 10^{16} cm).

c) Asymptotic Behavior

The behavior of $v_{p,n}$ as $s \to \infty$, 0 is best examined by considering the integrated form of the energy equation in the strong coupling limit, which is (along a flux tube)

$$M^2 - \ln M^2 - 4\ln y - \frac{4\bar{l}}{y} + \frac{\bar{\sigma}\lambda^2}{y^2}\left[1 + \frac{\left(2M_A^2 - 1\right)\left(1 - y^2/\lambda\right)^2}{\left(M_A^2 - 1\right)^2}\right] = \text{const}, \tag{67}$$

where $M = v_{p,n}/c_s$, $\bar{l} = GM_{\rm disk}/2r_0c_s^2$, and $\bar{\sigma} = (\alpha r_0)^2/c_s^2$. The asymptotic results evaluated from equation (67) are

© American Astronomical Society • Provided by the NASA Astrophysics Data System

1983ApJ...274..677P

then
(i) $y \to \infty$:

$$\begin{cases} M \ln M \approx \dfrac{\bar{\sigma}}{c} x^{|\nu|} \to \infty & (\nu < 0) \quad (68a) \\ M^2 \approx 4 \ln y \to \infty & (\nu > 0); \quad (68b) \end{cases}$$

$$M^2 \approx \exp\left(-\bar{\sigma} y^2\right) \to 0 \qquad (\text{all } \nu). \quad (68c)$$

(ii) $y \to 0$:

$$\begin{cases} M \ln M \approx \dfrac{\bar{\sigma}\lambda^2}{c} \dfrac{x^{|\nu|}}{y^4} \to \infty & (\nu < 0) \quad (68d) \\ M^2 \approx y^{-4} \to \infty & (\nu > 0); \quad (68e) \end{cases}$$

$$M^2 = \exp(-4\bar{l}/y) \to 0 \qquad (\text{all } \nu). \quad (68f)$$

The solution for supersonic winds is that inside the sonic point equation (68f) maintains, and beyond the magnetosonic point either equation (68a) or equation (68b) holds (depending on ν). Note that these solutions differ from the results of isothermal MHD flows with $\mathscr{A} \propto s^2$ only in the converging ($\nu < 0$) regime. From equation (68a) it is evident that much higher speeds are expected for the convergent outflows.

The solutions for M can be combined with the condition (51) for constant mass loss rates on a flux tube to determine ρ_n (i.e., $\rho_n \propto M^{-1}x^{-2k}$). This subsection is concluded by noting that, from equation (67), a value for λ can be found by evaluating the constant at the sonic and magnetosonic point of the flow, and then solving for λ (see GJ; Weber and Davis).

d) *Wind Energetics in Weak Coupling*

In weakly coupled flows, the control of the critical points depends crucially on the frictional heating effects. The second term in equation (48) is the frictional heating (depending on M) and acts to increase the gas pressure along the outflow. The competing term is the first term on the right-hand side of equation (48), which shows the increasing tendency of material to slip off the field lines as $r \to \infty$, and acts as a retarding agent to the flow. Thus, critical points are, in general, expected to occur but will not be investigated in this paper.

The next section will consider the character of the flow field inside the disk envelope, in order to understand how a flow along the disk's rotation axis could be initiated.

V. FLOW INITIATION IN THE DISK ENVELOPE

In this section we consider the question of how the outflow from the disk might be initiated. We will focus on the effects of magnetic flux loss by ambipolar diffusion out of the disk core into an extended disk envelope which has a large volume, but little mass compared to the core.

Mestel and Paris (1979) considered the effect of magnetic flux loss from a spherical cloud in approximate magneto-centrifugo-gravitational equilibrium. For a cloud held up by magnetic forces, flux loss by ambipolar diffusion will determine the contraction rate.

What happens in a flattened, rotating disk? We suppose that to first approximation the disk core and envelope are in equilibrium. For a flattened (axisymmetric) system, the drift of magnetic field and ions with respect to the neutrals is much more rapid in the vertical than in the radial direction [i.e., $v_z \approx O(v_r r/z)$], as will be seen shortly. Therefore, it is expected that a Poynting flux directed along the rotation axis of the disk will develop as a result of flux loss from a rotationally flattened disk. For a dense core of sufficiently low ionization fraction, the field and ions slip preferentially along the rotation axis. As this slipping field encounters the low density envelope, with sudden increase in x, it couples to the neutral gas and accelerates it.

The presence of an embedded protostar in the disk core is crucial in this view, because of its control over ionization in the core. When a protostar turns on, it will create a region of enhanced ionization in the core, with $\delta x/\delta z < 0$. Since the outward drift of field is proportional to x^{-1} (see below), it is evident that magnetic flux and ions drift out more quickly as they approach the core's outer edge. On encountering the envelope, this flux slams into the envelope gas and

© American Astronomical Society • Provided by the NASA Astrophysics Data System

1983ApJ...274..677P

may heat it significantly. In a self-consistent calculation it is expected that an envelope with a discontinuous increase in temperature and x, and a discontinuous drop in ρ_n, is formed. Notice that in the absence of an embedded star a dense disk will have $\delta x/\delta z > 0$, and outward leaking magnetic flux slows as it drifts. In this case, a disk envelope probably will not form.

Let us turn for a moment to the global view of this wind problem before elaborating upon the details of the previous paragraph. A centrifugally driven hydromagnetic wind stripping material away from the outer disk envelope will require some given pressure at the envelope base (as determined by evaluating eqs. [68] and [51] to calculate P at this point). This pressure may be maintained by heating the envelope in the manner just discussed. In this view, then, the disk adjusts to the demands of the centrifugal drive (determined once the coupling, β, and rotation, $v_{\phi,n}$, are known) by maintaining a disk envelope at the required pressure. Flux loss results in slow disk contraction, so that the gravitational potential energy released during this core contraction is the ultimate energy source for heating the envelope.

The final general point to consider is the fact that centrifugal driving requires the magnetic field lines to be appropriately shaped in order to intercept the gas on a favorable "track" (see Blandford and Payne for a discussion in the accretion disk context). The analysis of the previous section did not address this point. As long as the field is at least marginally coupled into the disk, the field lines will be shaped by the rotating, self-gravitating gas. This question is taken up at the end of this section.

To make the foregoing discussion concrete, consider the equation of motion for the whole fluid (add eqs. [5] and [6], with $x \ll 1$):

$$\boldsymbol{v}_n \cdot \nabla \boldsymbol{v}_n = -\frac{\nabla p_n}{\rho_n} - \nabla\Phi + \frac{(\nabla \times \boldsymbol{b}) \times \boldsymbol{b}}{4\pi\rho_n}. \tag{69}$$

A state of near magneto-centrifugo-gravitational balance will only be possible if the flux trapped in the disk exceeds some critical value, or, in terms of disk mass,

$$M \lesssim M_c = 140\, M_\odot \left(r_{\rm disk}/10^{17}\ {\rm cm}\right)^2 \left(b_{\rm disk}/10^{-3}\ {\rm G}\right).$$

Thus, the field threading the dense disk core ought to be of order a milligauss in strength. In this state, and for very small ionization fraction, the Lorentz force on the ions is balanced by frictional drag, so that (Mestel and Spitzer 1956)

$$-\boldsymbol{F}(\boldsymbol{v}) = \frac{(\nabla \times \boldsymbol{b}) \times \boldsymbol{b}}{4\pi}. \tag{70}$$

Equilibrium for the whole fluid (neglect $\boldsymbol{v}_{p,n}$ in eq. [69]), together with equations (70) and (7), allows us to solve for the components of the relative drift velocity:

$$\frac{v_z}{c_s} = -\tilde{\beta} z_0 \left(\frac{1}{\rho_n}\frac{\partial \rho_n}{\partial z} + \frac{1}{c_s^2}\frac{\partial \Phi}{\partial z} \right), \tag{71a}$$

$$\frac{v_r}{c_s} = -\tilde{\beta} z_0 \left(\frac{1}{\rho_n}\frac{\partial \rho_n}{\partial r} + \frac{1}{c_s^2}\frac{\partial \Phi}{\partial r} - \frac{v_{\phi,n}^2}{c_s^2}\frac{1}{r} \right),$$

$$\tilde{\beta} \equiv c_s/x\rho_n\eta_{in}z_0, \tag{71b}$$

where z_0 is the local disk scale height, and where, for convenience, we have specialized to an isothermal gas. The result (71) shows that in flattened systems the vertical field drift is at least a factor of r/z_0 larger than the radial drift speed, so that the field and ions are behaving like a buoyant fluid in the disk. The second point about equation (71) is that $v \propto x^{-1}$, so that the outward drift accelerates as x decreases (as when a protostar is embedded in the disk core).

The question now arises as to what is the shape of the field lines at the base of the disk envelope. Only if the field lines make a sufficiently small angle with respect to the disk core surface will the centrifugal force be able to accelerate gas out of the system by attachment to the field lines.

The shape of the field lines can be determined from equations (71a), (71b). Provided that we are in the regime where $v_p/c_s \ll \beta(\Phi - \int v_\phi^2/r\,dr)/c_s^2$, which will be valid close to the disk core surface, far away from any critical points in the

© American Astronomical Society • Provided by the NASA Astrophysics Data System

1983ApJ...274..677P

outgoing wind, then, since $v_{p,i} = \kappa b_p$, the ratio of equations (71a), (71b) gives the equation for the field lines:

$$(dz/dr)_{\text{field line}} \approx \left[\rho_n^{-1}\frac{\partial \rho_n}{\partial z} + c_s^{-2}\frac{\partial \Phi}{\partial z}\right]\left[\rho_n^{-1}\frac{\partial \rho_n}{\partial r} + c_s^{-2}\left(\frac{\partial \Phi}{\partial r} - \frac{v_{\phi n}^2}{r}\right)\right]^{-1}. \tag{72}$$

Note that $b_z/b_r = dz/dr$. Equation (72) conceals the fact that if the magnetic field is important for disk structure, then ρ_n, Φ, and $v_{\phi,n}$ are implicit functions of the field.

Analysis of equation (72) is easier in the disk envelope because Φ may be taken to arise from the massive core. In addition, inside the envelope, far from any critical points in the wind, the field is primarily poloidal, and therefore $v_{\phi,n}$ may be taken to be independent of b_ϕ in this zone only.

To return to equation (72), it is useful to introduce the effective gravitational potential

$$U \equiv \Phi - \int \Omega^2 r\, dr. \tag{73}$$

It is important to emphasize that for an equation of state $p = p(\rho)$, by von Zeipel's theorem, $\Omega = \Omega(r)$ (see, e.g., Paczyński and Wiita 1980). With this result, equation (72) takes the form

$$\left(\frac{dz}{dr}\right)_{\text{field line}} = \frac{\partial x}{\partial z} \Big/ \frac{\partial x}{\partial r},$$

$$X \equiv \frac{U}{c_s^2} + \ln \rho_n. \tag{74}$$

Therefore, the *field lines* define surfaces on which, from equation (74),

$$\nabla\left(U + c_s^2 \ln \rho_n\right) \times (d\boldsymbol{x})_{\text{field line}} = 0, \tag{75}$$

$$\boldsymbol{x} = (r, z).$$

Contrast this result with the equation governing the surface of equilibrium for the rotating, self-gravitating core

$$dU = \nabla U \cdot (d\boldsymbol{x})_{\text{surface}} = 0. \tag{76}$$

Comparison of equations (76) and (75) shows that in the absence of pressure effects, the field lines emerge *perpendicular* to the disk core surface. Gas pressure will, however, bend the field lines away from perpendicular emergence, as shown in equation (75). This is an important point. The pressure of the envelope will bend the field lines, which affects the efficiency of the centrifugal drive. We speculate that a completely self-consistent analysis would show a self-regulating step here. The demands of the disk wind would provide an appropriately tailored field line curvature by control of the envelope pressure.

Far enough along the disk surface, the field lines will be insufficiently distorted from their parallel alignment to the rotation axis to serve as paths along which gas may be accelerated away from the core by centrifugal forces. In this region, then, we suspect that gas in the envelope will slowly settle onto the disk, rather than be moved outward by the centrifugal drive. Figure 1 gives a cartoon approximation of the situation we have in mind.

We close this section by recalling the point we made in the beginning. If it is supposed that radiative heating of an envelope is insufficient to provide the required pressure at the base of the wind, it remains to be shown how magnetic processes could do this. This has been the intent of this section, which borrows from the suggestions Mestel and Paris made some time ago. We turn now to discuss the implications of this analysis.

VI. IMPLICATIONS

In this section, we discuss some of the main consequences of the picture of centrifugally driven winds from contracting disks, both for observational efforts, and for the physics of molecular clouds in general.

a) Magnetic Braking and Star Formation Efficiency

The efficiency of magnetic braking depends upon the coupling parameter β and manifests itself as the degree to which the field lines slip with respect to the neutral gas. Given a cloud density and flow time scale, the ionization

© American Astronomical Society • Provided by the NASA Astrophysics Data System

1983ApJ...274..677P

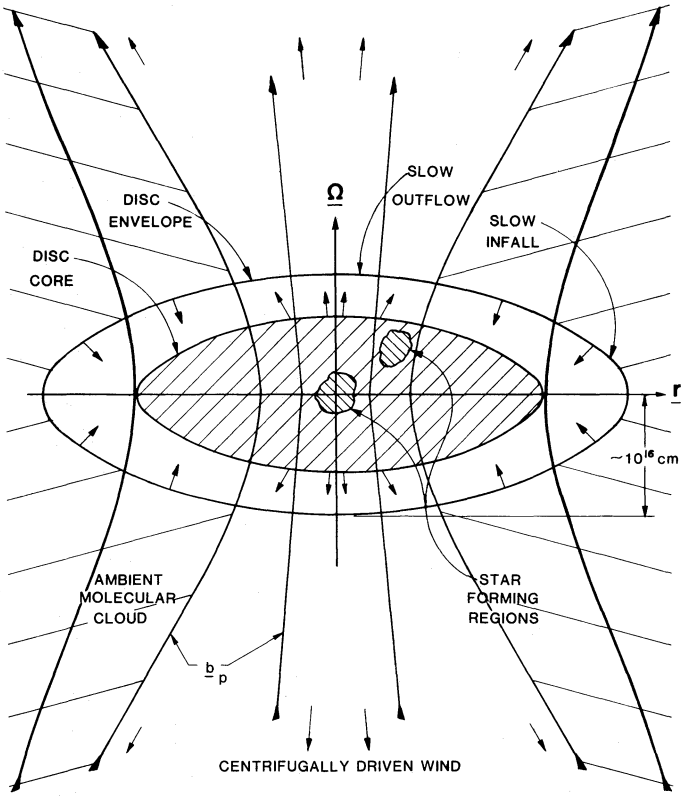

FIG. 1.—Cartoon depicting a molecular disk near magneto-centrifugo-gravitational equilibrium which is driving (centrifugally) a wind up the rotation axis. Flux loss from the flattened core is mainly along the rotation axis of the disk, and, when a protostar forms, the Poynting flux is sufficient to heat the disk envelope. The disk core continuously contracts as magnetic flux leaks away. Sufficiently far from the rotation axis, material from the surrounding molecular cloud may settle onto the envelope.

fraction determines β ($\beta \propto x^{-1}$). For molecular clouds with $n_n \approx 10^6$, $v_{p,n} \approx 10^6$ cm s^{-1} over scales $\sim 10^{17}$ cm, $\beta \approx 10^{-8}/x$; if $x \approx 10^{-7}$, the bipolar outflow would be strongly coupled to about an order of magnitude ($\beta \approx 10^{-1}$). We suggest that the outflow is activated when a protostar begins to alter the ionization state of the embedding molecular disk. Before protostellar birth, clouds may be only marginally coupled ($\beta \approx 1$), so that angular momentum is not easily shed. Star formation efficiency would be low in such a cloud. When a protostellar core turns on, it could trigger an era of strongly coupled, angular momentum shedding by a wind, which reduces the "angular momentum problem" in the disk and allows subsequent star formation in the region to be far more efficient. The basic criterion to be met is that the Strömgren sphere of a newly formed O star should envelope a neighboring protostellar region. This will be particularly possible in a two-phase cloud model with stars forming close to the edge.

b) Existence of Dense Molecular Disk

If magnetic braking is inefficient (marginal coupling in the absence of young stars), then rotationally supported, molecular disks ought to be fairly common. Stars would be unable to form in such disks because the density is too low and the angular momentum excessive. As soon as a few stars do manage to form, an era of rapid angular momentum shedding might be initiated (manifested as the bipolar outflows). In order for stars to form, magnetic flux loss must also occur, and so we suspect that although the coupling ought to be strong, it should not be so strong that magnetic flux does not leak out of the disk. Indeed, we have argued that this flux loss ultimately provides an envelope of the pressure required to feed the centrifugally driven wind. Angular momentum loss and ambipolar effects operate very closely together in our scheme.

© American Astronomical Society • Provided by the NASA Astrophysics Data System

1983ApJ...274..677P

c) *Environmental versus Self-regulatory Effects*

Since the specific angular momentum of a cloud depends upon how much star formation has occurred (see §§ VI*a*, *b*), it is expected that the most recently formed stars are considerably slower rotators than the oldest stellar population in the disk. Such an age-rotation correlation ought to be observable in a cluster of newly formed stars.

The second major issue hinges on the fact that the amount of angular momentum carried out by the wind depends upon the degree of field line slip at the Alfvénic point (see § IV). Thus, β_{r_A} is crucial. Two very different mechanisms may control the ionization state of the outflow at the crucial Alfvénic radius and are (i) environmental and (ii) self-regulatory. If x_{r_A} is environmentally controlled, then it is expected that star formation is far more efficient near the edges of giant molecular clouds. The reason is that here the ionization fraction x is much higher because of external sources of ionizing photons (this also holds for the edges of subclumps or subclouds of which a GMC may be constituted). The other possibility for the flow is that x_{r_A} is regulated by the flow and/or protostar alone. As an example, if ions are dredged up from the ionized zone about the protostar or disk envelope and carried out by the flow, the wind may be able to control x_{r_A} very effectively. In this case, star formation efficiency may be just as high in the deep interior of dense GMCs as near their surfaces. Perhaps the fact that the wind in L1551 which occurs deep in a dense dark nebula, and Orion, which borders on a famous H II region, are both very energetic flows is an example of possible self-regulatory behavior in action.

d) *Wind Characteristics*

We have noted that when a protostar turns on, it will provide a zone of ionization which ought to couple the neutral gas to the field more effectively than before. An epoch of efficient angular momentum shedding may now begin. As discussed in § V, it is expected that a disk envelope forms as well, with a pressure sufficient to maintain the centrifugally driven wind that now forms. This envelope may be thought of as a disk "corona" which is heated by emergent magnetic flux from the core. In a different context, Blandford and Payne (1982) discussed the role of a disk corona for centrifugally driven winds from accretion disks.

The general structure of the magnetic field is important for determining wind characteristics. As seen in § IV, if flux tubes open up faster than $\mathscr{A} \propto s^2$, the sonic point occurs closer to the disk surface for slowly rotating disks. This is very important physically because the activation energy for the wind can be deposited in the disk envelope, rather than farther out in the flow.

As already discussed, the symmetry axis for a flow off the disk ought to be that of the disk's rotation axis. The most massive young star will be formed on the disk axis. If further star formation occurs, these may not be so aligned. The role of the young stars, as far as wind formation is concerned, is to provide the appropriate ion gradient and activation energy for the cold MHD wind.

An important features about magnetic winds is that ion species can be differentiated in a way that is distinguishable from the radiatively driven wind. The longer the gyroradius of a charged particle in the field, the more efficiently it is accelerated, until a particle cannot complete a gyration before it undergoes a collision. The requirement for acceleration then is that the gyrofrequency ($\omega_H = eb/m_i c$) be larger than the particle's collision frequency with the neutrals ($\nu_{in} = \rho_n \eta_{in}$), i.e.,

$$A/z < (A/z)_c = 10^2 (b/10^{-5}\ \mathrm{G})(n_n/10^6\ \mathrm{cm}^{-3})^{-1}. \tag{77}$$

Thus, most atomic ions (O^+, Ca^+, etc.) ought to be efficiently accelerated, but heavy grains ($M_{\mathrm{grain}} \approx 10^8\ M_P$) will not. Furthermore, for $A/z < (A/z)_c$, the particles with higher charge-to-mass ratios will be more efficiently accelerated, and hence depleted, with respect to the depletion seen in the light ion species (H_2^+, etc.). It should be noted that this relative depletion of heavy ions has been studied in the case of the polar wind from the Earth's ionosphere (see, e.g., Banks and Holzer 1969).

It is important to note that when the ionization fraction is less than $\sim 5 \times 10^{-8}$, grain-thermal viscosity can exceed the ion-neutral viscosity (Elmegreen 1979). Effectively, the dynamics of the negatively charged grains then controls the coupling of the field to the neutrals. We conjecture that for weakly coupled flows in dense molecular clouds ($x \leq 10^{-8}$), the dynamics of the negatively charged grains essentially controls the character of the hydromagnetic flow.

e) *Magnetic Fields*

As discussed in the introduction, the molecular disk is assumed to be a compressed oblate gas with the rotation axis aligned with the magnetic axis. The wind will open out this field as it leaves the disk. Beyond the critical points in the supersonic flow regime, the Chan and Henricksen (1980) mechanism of flow collimation by magnetic hoop stress may come into play. Far beyond the position of the shock (≥ 1 pc) in which the wind rams the external cloud medium, the field lines ought to join smoothly into a bundle along which the material in the molecular disk originally contracted.

© American Astronomical Society • Provided by the NASA Astrophysics Data System

1983ApJ...274..677P

It was noted in § IV that higher speed flows at the disk surface are expected for more rapid flux tube divergence. In § V it was shown that the field as it leaves the disk core is shaped by the effective gravity and pressure effects such that for negligible gas pressure, the field lines would emerge perpendicular to surfaces of constant effective gravity.

f) *Observational Implications*

1. Existence of molecular disks of mass $M \approx 100\ M_\odot$ on scales $\sim 10^{16}$ cm, "impaled" on galactic magnetic field lines in such a way that the disk rotational and magnetic axes are aligned has been established. The characteristic double profile in CO corresponding to a cool rotating molecular disk should be searched for.
2. There exists an angular momentum-age sequence for stars forming in the disk region such that the youngest stars should have the smallest specific angular momentum.
3. The wind flow axis ought to be that of the disk, and not necessarily be aligned with the young star(s) in the disk.
4. A separation of ion species by mass-to-charge ratio should occur. Thus, heavier ion species should be more depleted than light ion species. Grains will not be accelerated.
5. The molecular disk ought to be comprised of a dense core surrounded by a low mass, more highly ionized envelope.
6. If the ionization fraction x in the wind is primarily externally controlled, then magnetic braking efficiency, and hence star formation efficiency, may be greater for massive stars forming near the edge of giant molecular clouds or subclouds rather than deep inside their denser cores.
7. These protostellar disks with their centrifugally driven winds could be a significant energy input into the molecular clouds, providing an additional source of turbulent energy (Norman and Silk 1980).
8. Further observations of debris in the wind associated with masers and Herbig-Haro objects may help discriminate various flow models (Norman and Silk 1979; Elmegreen and Morris 1979; Genzel and Downes 1977; Morris, Bower, and Turner 1982).

VII. CONCLUSIONS

The main results of our work are the following:

1. The key parameter in partially ionized clouds that determines the characteristics of MHD flows is the coupling parameter $\beta = T_{n-i}/T_{\rm fl}$.
2. For strongly coupled flows ($\beta \ll 1$) the neutrals, ions, and field move together. Bipolar outflows in molecular clouds may be strongly coupled to about an order of magnitude ($\beta \approx 10^{-1}$) for $x \approx 10^{-7}$.
3. The efficiency of angular momentum transport depends on the coupling. In the strongly coupled limit, the efficiency of angular momentum transport is reduced by the factor $(1-\beta)_{r_A}$ which is determined at the Alfvénic point.
4. Strongly coupled flows can be quite steady. Highly variable flow may occur in the weakly coupled limit.
5. If bipolar molecular flows are strongly coupled, centrifugally driven winds from molecular disks, then for a wind mass loss of $\dot{M}_{\rm wind} \approx 10^{-4}\ M_\odot\ {\rm yr}^{-1}$, the Alfvénic radius of the flow is at $\sim 10^{17}$ cm. The underlying disk ought to have a scale $\leq 10^{16}$ cm, mass $M_{\rm disk} \approx (1-\beta)_{r_A}^{-1}\ 100\ M_\odot$, and core magnetic field $\sim 10^{-3}$ gauss. The disk will have to have rotational velocities of $\sim 10^6$ cm s^{-1} to explain the most energetic outflows of $\sim 10^{47}$ ergs. The sonic point will occur just at the top of the disk envelope for the rapid rotators.
6. Frictional heating is an $O(\beta)$ effect in strongly coupled regimes.
7. The position of critical points in a strongly coupled outflow depends on flux tube divergence. If the flux tube cross-sectional area diverges faster than $\mathscr{A} \approx s^2$, the sonic point lies closer to the disk (for slow rotators), and the outflow is faster.
8. As long as the underlying disk is in approximate magneto-centrifugo-gravitational balance, slow flux loss from the core "heats" a disk envelope when a protostar forms.
9. The outflow in the disk envelope (under isothermal conditions) is a doubly opposed cone about the disk rotation (and magnetic) axis.
10. Magnetized winds will show a velocity dispersion for the ions which increases with A/z until some critical value $(A/z)_c \approx 100$. Thus, heavier ion species [with $A/z < (A/z)_c$] ought to be more depleted than lighter species.

We are particularly grateful to Jon Arons, Arieh Königl, and Chris McKee for discussions which have greatly enhanced the content of this paper, and thank Bruce Elmegreen for insightful refereeing. R. E. P. thanks Sterrewacht, Leiden for hospitality enjoyed while some of this work was in progress and acknowledges financial support of a Canadian NSERC postdoctoral fellowship and NSF grant AST 79-23243 to the University of California at Berkeley.

© American Astronomical Society • Provided by the NASA Astrophysics Data System

1983ApJ...274..677P

APPENDIX

FAST RECOMBINATION LIMIT

The basic results for fast recombination limit flows are outlined. The main technical difficulty here is that $\rho_i\kappa$ is no longer a constant along field lines and is instead

$$\boldsymbol{b}\cdot\nabla(\kappa\rho_i) = S_i. \tag{A1}$$

The angular momentum equation for the ion fluid then becomes

$$\boldsymbol{b}\cdot\nabla(L) = \frac{1}{\kappa\rho_i}\left(rF_\phi - \frac{rb_\phi}{4\pi\kappa\rho_i}S_i\right) \tag{A2}$$

which may be compared with equation (21). Thus, changing the ionization state of the fluid as it moves along changes the "ion loading" of a field line. This changing inertia induces a torque on the fluid.

An explicit solution for b_ϕ can be found. In the *strong coupling limit*, the angular momentum equation for the whole fluid will take the form $\boldsymbol{b}\cdot\nabla(L) = -(\rho_n\kappa)^{-1}rS_ib_\phi/4\pi\kappa\rho_i$, where L is given by equation (31). So with equation (16) it is found that

$$\frac{db_\phi}{ds} + \lambda b_\phi = G, \tag{A3}$$

where

$$\lambda \equiv \frac{(rS_i/\rho_n v_{p,n}4\pi\kappa\rho_i)}{y} + \frac{d}{ds}(\ln y)$$

$$\equiv \frac{\mathscr{S}_i}{y} + \frac{d}{ds}(\ln y), \tag{A4}$$

with

$$y \equiv \frac{\kappa r}{(1+\beta)}\left[1 - \frac{(1+\beta)}{4\pi\kappa^2\rho_n}\right], \tag{A5}$$

$$G \equiv \left(-\frac{1}{y}\right)\frac{d}{ds}\left(\frac{\alpha r^2}{1+\beta}\right) \equiv \mathscr{G}/y. \tag{A6}$$

The solution is then

$$b_\phi = \frac{1}{y}\exp\left(-\int\frac{\mathscr{S}_i}{y}ds\right)\left[\tilde{L} + \int\mathscr{G}\exp\left(+\int\frac{\mathscr{S}_i}{y}ds\right)ds\right], \tag{A7}$$

where $\tilde{L}$ is the constant of integration. In the case $\mathscr{S}_i = 0$, equation (A7) readily reduces to equation (33). The Alfvénic point (where $y = 0$) is the same condition as in the slow recombination case. The value for $\tilde{L}$ at the point, however, now depends on $(S_i)_{r_A}$ in a somewhat more complicated way. The general result that the field line slip at the Alfvénic point determines $\tilde{L}$ still holds. The ionization state at the Alfvénic radius, which determines this slip, now has an additional contribution from S_i.

Finally, the energy equation for the ions is now

$$\nabla\cdot(\rho_i\mathbf{v}_i\mathscr{E}_i) = \mathbf{v}_i\cdot\mathbf{F} + \frac{r\alpha b_\phi S_i}{4\pi\kappa\rho_i} \tag{A8}$$

which shows that the torque induced by the changing ion inertia on a field line (measured by S_i) does work on the ion fluid. The energy equation for the total fluid is modified by the addition of $r\alpha b_\phi S_i/4\pi\kappa\rho_i$ to the frictional heating term.

© American Astronomical Society • Provided by the NASA Astrophysics Data System

1983ApJ...274..677P

REFERENCES

Banks, P. M., and Holzer, T. E. 1969, *J. Geophys Res.*, **74**, 6317.
Blandford, R. D., and Payne, D. G. 1982, *M.N.R.A.S.*, **199**, 883.
Chan, K. L., and Henricksen, R. N. 1980, *Ap. J.*, **241**, 534.
Chandrasekhar, S. 1956, *Ap. J.*, **124**, 232.
de Jong, T., Chu, S-I., and Dalgarno, A. 1975, *Ap. J.*, **199**, 69.
Downes, D., Genzel, R., Becklin, E. E., and Wynn-Williams, C. G. 1981, *Ap. J.*, **244**, 869.
Elmegreen, B. G. 1979, *Ap. J.*, **232**, 729.
Elmegreen, B., and Morris, M. 1979, *Ap. J.*, **229**, 593.
Genzel, R., and Downes, D. 1977, *Astr. Ap. Suppl.*, **30**, 145.
Goldreich, P., and Julian, W. H. 1970, *Ap. J.*, **160**, 971 (GJ).
Hartmann, L., and MacGregor, K. B. 1982, *Ap. J.*, **259**, 180.
Henricksen, R. N., and Rayburn, D. R. 1971, *M.N.R.A.S.*, **152**, 323.
Hollenbach, D., and McKee, C. F. 1979, *Ap. J. Suppl.*, **41**, 555.
Holzer, T. E. 1977, *J. Geophys Res.*, **82**, 23.
Königl, A. 1982, *Ap. J.*, **261**, 115.
Krall, N. A., and Trivelpiece, A. W. 1973, *Principles of Plasma Physics* (New York: McGraw-Hill).
Kwan, J., and Scoville, N. J. 1976, *Ap. J.* (*Letters*), **210**, L39.
Lada, C. J., and Harvey, P. M. 1981, *Ap. J.*, **245**, 58.
Mestel, L. 1961, *M.N.R.A.S.*, **122**, 473.
_____. 1968, *M.N.R.A.S.*, **138**, 359.
Mestel, L., and Paris, R. B. 1979, *M.N.R.A.S.*, **187**, 337.
Mestel, L., and Spitzer, L. Jr. 1956, *M.N.R.A.S.*, **116**, 503.
Morris, M., Bower, P. F., and Turner, B. E. 1982, *Ap. J.*, **259**, 625.
Mouschovias, T. Ch. 1976, *Ap. J.*, **207**, 141.
_____. 1981, in *IAU Symposium 93, Fundamental Problems in the Theory of Stellar Evolution*, ed. D. Sugimoto, D. Q. Lamb, and D. N. Schramm (Boston: Reidel), p. 27.
Mouschovias, T. Ch., and Paleologou, E. V. 1980, *Ap. J.*, **237**, 877.
_____. 1981, *Ap. J.*, **246**, 48.
Norman, C., and Silk, J. 1979, *Ap. J.*, **228**, 197.
_____. 1980, *Ap. J.*, **238**, 158.
Oppenheimer, M., and Dalgarno, A. 1974, *Ap. J.*, **192**, 29.
Paczyński, B., and Wiita, P. J. 1980, *Astr. Ap.*, **88**, 23.
Scoville, N. Z. 1981, in *IAU Symposium 96, Infrared Astronomy*, ed. C. G. Wynn-Williams and D. P. Cruikshank (Boston: Reidel), p. 187.
Snell, R. L., and Edwards, S. 1981, *Ap. J.*, **251**, 103.
Snell, R. L., Loren, R. B., and Plambeck, R. L. 1980, *Ap. J.* (*Letters*), **239**, L17.
Spitzer, L., Jr. 1978, *Physical Processes in the Interstellar Medium* (New York: Wiley-Interscience).
Thaddeus, P. 1977, in *IAU Symposium 75, Star Formation*, ed. T. de Jong and A. Maeder (Boston: Reidel), p. 37.
Vrba, F. J., Strom, S. E., and Strom, K. M. 1976, *A.J.*, **81**, 958.
Weber, E. J., and Davis, L., Jr. 1967, *Ap. J.*, **148**, 217.

C. A. NORMAN: Institute of Astronomy, Madingley Road, Cambridge CB3 OHA, England, UK

R. E. PUDRITZ: Department of Astronomy, University of California, Berkeley, CA 94720

© American Astronomical Society • Provided by the NASA Astrophysics Data System